Hybrid Dielectric Materials for Device Technologies: *Understanding Relationships between Molecular Structure and Properties*

Karsu I. Kilic and Reinhold H. Dauskardt
Materials Science and Engineering
Stanford University

8 Industry Liaisons, including:
INTEL, IBM, TSMC, Samsung

This work was supported by Semiconductor Research Corporation (SRC) Program under task ID 2957.001.

Stanford | ENGINEERING

1

Low-Dielectric Constant Hybrid Organosilicate Glasses

microelectronics | light weighting | display | flexible | solar | protective

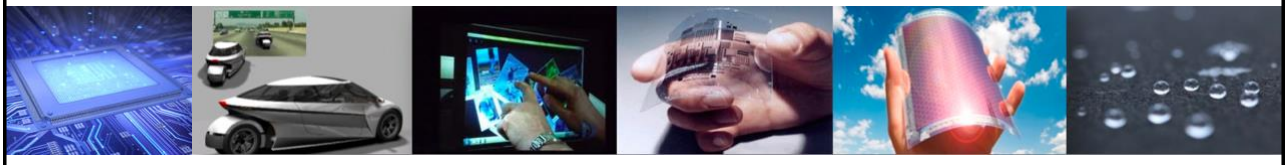

Nanoscale Confinement of Low-k Dielectric in Interconnect Devices

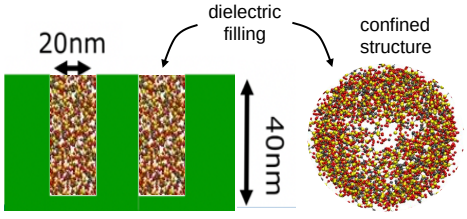

Application to other areas involving open-air spray-plasma deposition

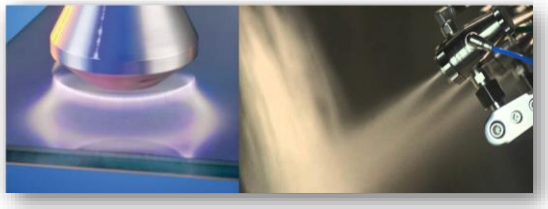

Stanford | ENGINEERING

2

Molecular Modeling of Hybrid Dielectric Materials

Simulation Elements

Oxygen:

OCS:

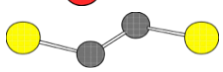

H atoms are modeled implicitly (united atom approach)

Bonded Interactions

$$U(r) = k(r - r_0)^2$$ (parameterized using ab-initio methods)

$$U(\theta) = k(\theta - \theta_0)^2$$

$$U(\phi) = \frac{1}{2}K_1[1 + \cos\phi] + \frac{1}{2}K_2[1 - \cos 2\phi] + \frac{1}{2}K_3[1 + \cos 3\phi] + \frac{1}{2}K_4[1 - \cos 4\phi]$$

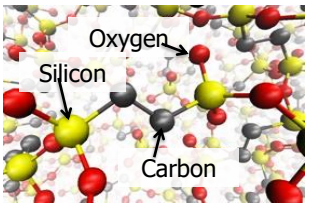

Non-Bonded Interactions

Stillinger-Weber Potential

$$U = \sum_i \sum_{j>i} \phi_2(r_{ij}) + \sum_i \sum_{j\neq i} \sum_{k>j} \phi_3(r_{ij}, r_{ik}, \theta_{ijk})$$

$$\phi_2(r) = A\epsilon\left[B\left(\frac{\sigma}{r}\right)^p - \left(\frac{\sigma}{r}\right)^q\right]\exp\left(\frac{\sigma}{r - a\sigma}\right)$$

$$\phi_3(r, s, \theta) = \lambda\epsilon\left[\cos\theta - \cos\theta_0\right]^2 \exp\left(\frac{\gamma\sigma}{r - a\sigma}\right)\exp\left(\frac{\gamma\sigma}{s - a\sigma}\right)$$

Reactive Force Potentials

$$E_{system} = E_{bond} + E_{over} + E_{under} + E_{lp} + E_{val} + E_{pen} + E_{tors} + E_{conj} + E_{vdWaals} + E_{Coulomb}$$

(With the inclusion of H atoms)

Ters-off Potential

$$E = \sum_i E_i = \frac{1}{2}\sum_{i\neq j} V_{ij}$$

$$V_{ij} = f_c(r_{ij})[f_R(r_{ij}) + b_{ij} f_A(r_{ij})]$$

$$f_R(r_{ij}) = A_{ij}\exp(-\lambda_{ij} r_{ij})$$

$$f_A(r_{ij}) = B_{ij}\exp(-\mu_{ij} r_{ij})$$

$$f_c(r_{ij}) = \begin{cases} 1, & r_{ij} < R_{ij} \\ \frac{1}{2} + \frac{1}{2}\cos\left(\pi\frac{r_{ij} - R_{ij}}{S_{ij} - R_{ij}}\right), & R_{ij} < r_{ij} < S_{ij} \\ 0, & r_{ij} > S_{ij} \end{cases}$$

$$b_{ij} = \chi_{ij}(1 + \beta_i^{n_i}\zeta_{ij}^{n_i})^{-1/2n_i}$$

$$\zeta_{ij} = \sum_{k\neq i,j} f_c(r_{ik})\omega_{ik} g(\theta_{ijk})$$

$$g(\theta_{ijk}) = 1 + \frac{c_i^2}{d_i^2} - c_i^2/[d_i^2 + (h_i - cos\theta_{ijk})^2]$$

$$\lambda_{ij} = (\lambda_i + \lambda_j)/2,\ \mu_{ij} = (\mu_i + \mu_j)/2$$

$$A_{ij} = (A_i + A_j)/2,\ B_{ij} = (B_i + B_j)/2$$

$$R_{ij} = (R_i R_j)^{1/2},\quad S_{ij} = (S_i S_j)^{1/2}$$

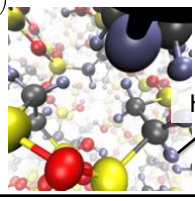

Initial Random Configuration

Final Low Energy Configuration

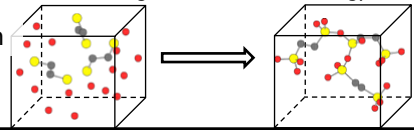

Stanford | ENGINEERING

3

3

Precursors with Different Molecular Geometry and Connectivity

All modeled with Hartree-Fock Ab-initio simulations for molecular structure and optimized bonded potentials.

precursor chain length

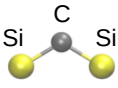

Si-Si distance

3 Å

4.5 Å

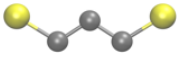

5.5 Å

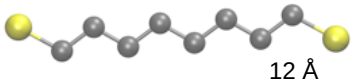

12 Å

precursor planarity

1,3,5-benzene (10º)

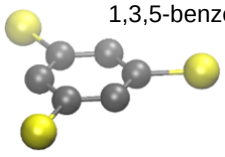

1,3,5-cyclohexane (20º)

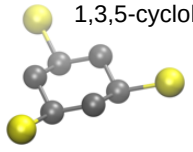

1,2,3-cyclopropane (50º)

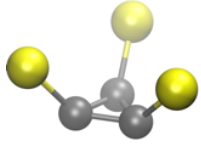

precursor connectivity (mSi)

Et-OCS (4)

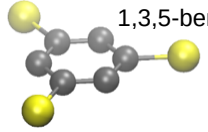

1,3,5-benzene (5)

1,2,5,6-pentalene (6)

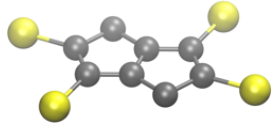

Stanford | ENGINEERING

4

Design of Ultrastiff Low-k Hybrid Organosilicate Glasses

Network Connectivity

$mSi_{max} = 4$ $mSi_{max} = 5$

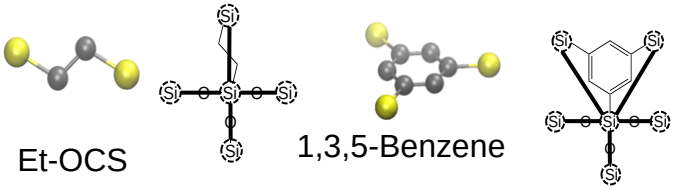

Et-OCS 1,3,5-Benzene

Precursor Geometry

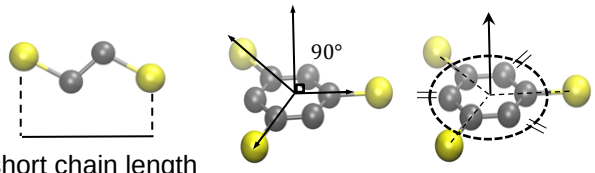

short chain length planar centrosymmetric

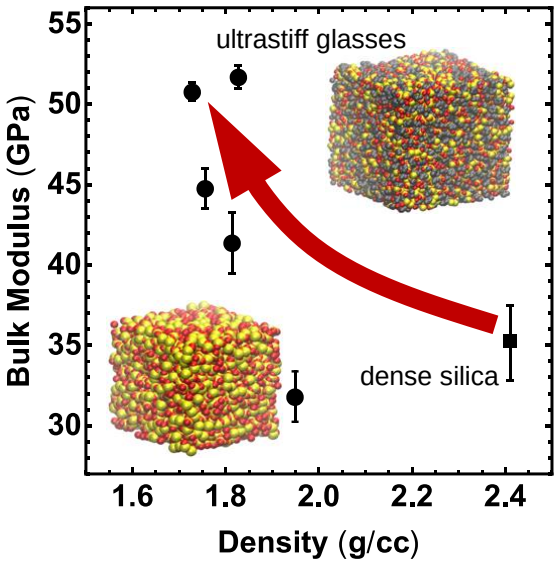

Stanford | ENGINEERING

K.I. Kilic & R.H. Dauskardt, *Advanced Functional Materials*, 2019.

5

Simulating the Fracture Properties with Graph Theory

decompose network and compute bonds | transform to weighted graph | min-cut algorithm | compute fracture height, cohesion, etc.

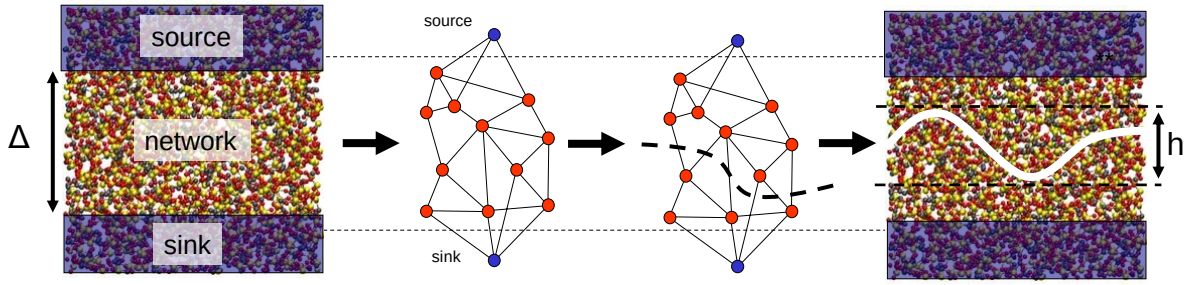

$$G_C\left[\frac{energy}{area}\right] = \underbrace{\frac{bonds}{area}}_{\text{min-cut}}\frac{energy}{bond}$$

Stanford | ENGINEERING

6

Simulating the Fracture Properties with Graph Theory

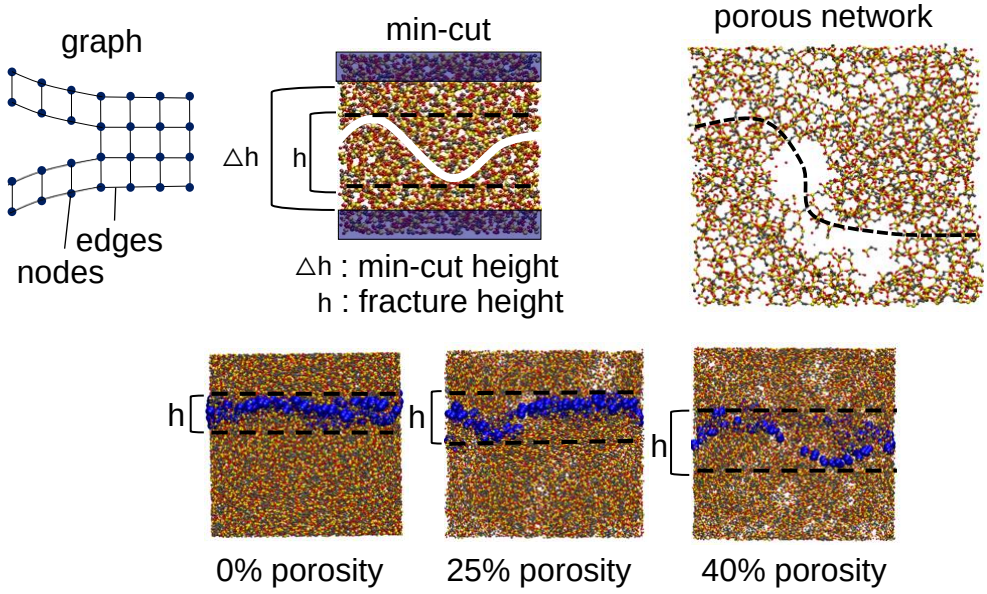

Stanford | ENGINEERING

Kilic et al., Mechanically reliable hybrid organosilicate glasses for advanced interconnects, Journal of Vacuum Science & Technology B, (2020).

7

Hyperconnected Planar Precursors Enhance Elastic and Fracture Properties

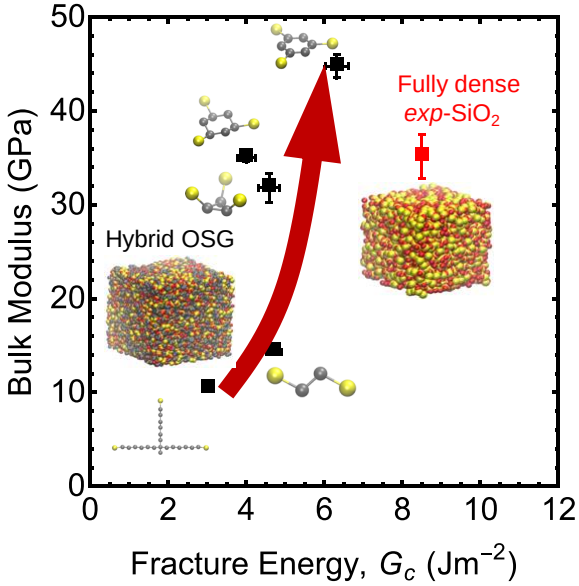

Cyclic Organic Chains

Hyperconnected (mSi_{max} = 5)

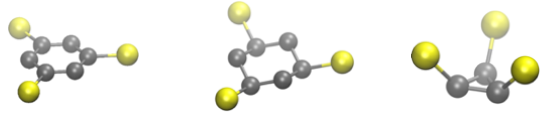

1,3,5-benzene 1,3,5-cyclohexane 1,2,3-cyclopropane

Acyclic Organic Chains

Conventionally connected (mSi_{max} = 4)

Hyperconnected (mSi_{max} = 5)

Et-OCS

Flexible silane R_6

R = CH_2

Stanford | ENGINEERING

Kilic et al., Mechanically reliable hybrid organosilicate glasses for advanced interconnects, Journal of Vacuum Science & Technology B, (2020).

8

Experimental Results for the low-k Hybrid OSG Networks

Elastic Properties

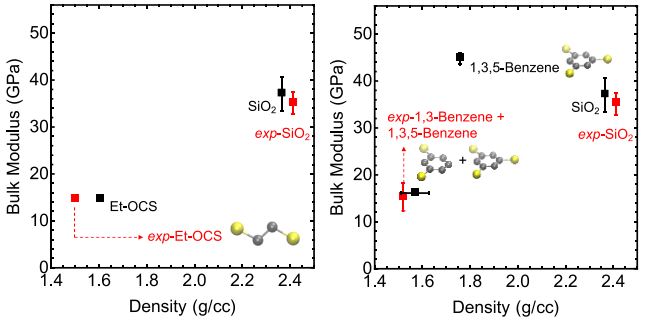

Dielectric Properties

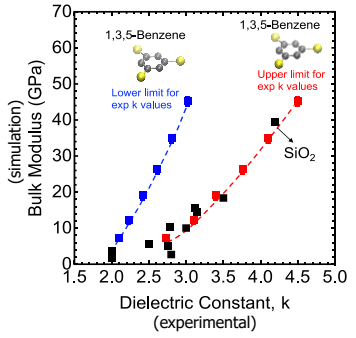

Fracture Properties

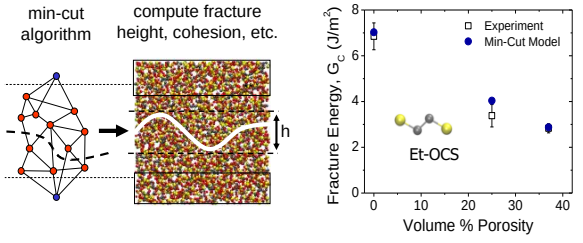

Stanford | ENGINEERING

Rasadujjaman et al., Analytical Study of Porous Organosilicate Glass Films Prepared from Mixtures of 1,3,5- and 1,3-Alkoxysilylbenzenes, Materials, 2021.
Liu et al., Properties of organosilicate low-k films with 1,3- and 1,3,5-benzene bridges between Si atoms, Japanese Journal of Applied Physics, 2020.
Burg et al., Hyperconnected molecular glass network architectures with exceptional elastic properties, Nature Comm. (2017)

9

Effects of Nanoscale Device Confinement

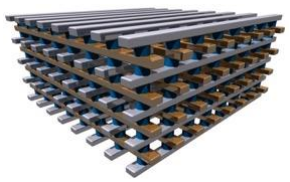

Predicting the role of nano-scale geometrical cofinement on the structure and mechanical reliability of hybrid organosilicate materials

Relevant Trench Geometries

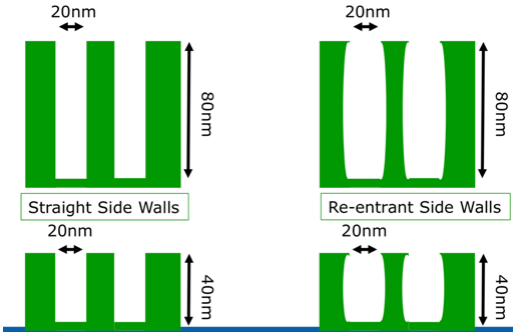

Low-k dielectric hybrid organosilicate network

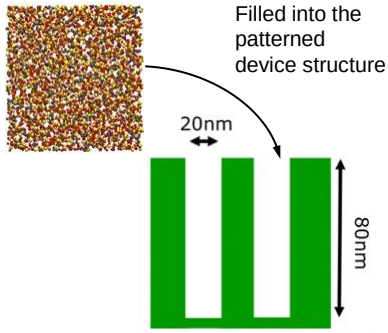

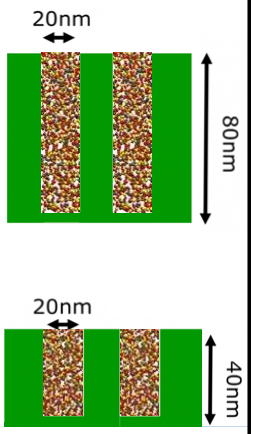

Stanford | ENGINEERING

10

Methodology to Simulate Nanoconfinement Effects

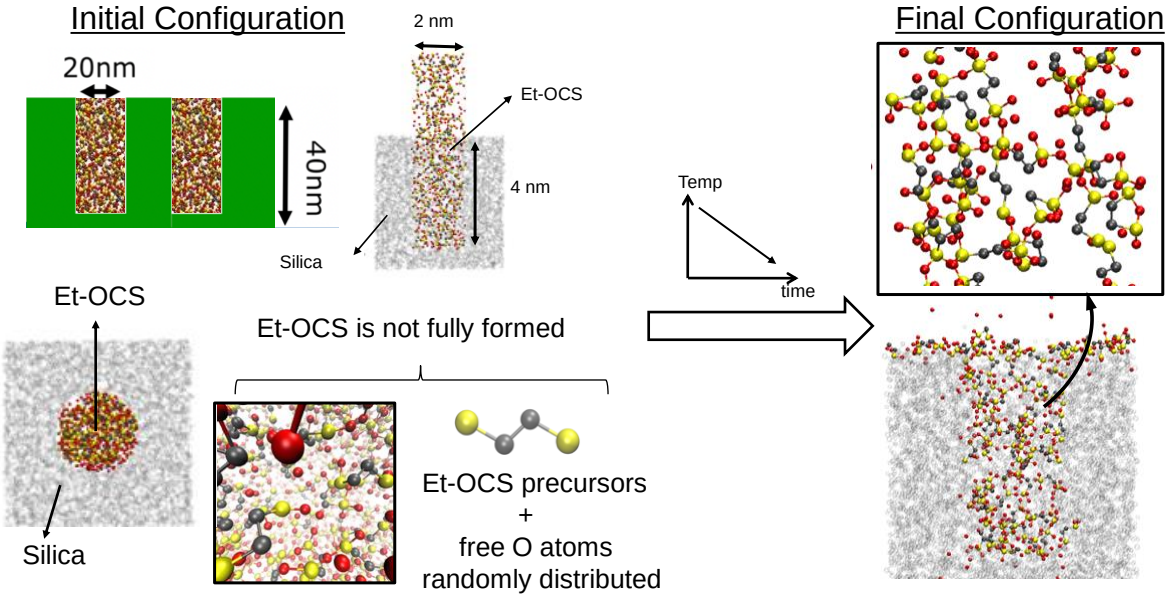

Stanford | ENGINEERING

Kilic et al., Computational Analysis of the Role of Nanoconfinement on the Reliability of ULK Glasses, *Proceedings of IEEE* (IITC), 2022.

11

Effects of Nanoconfinement At Different Scales

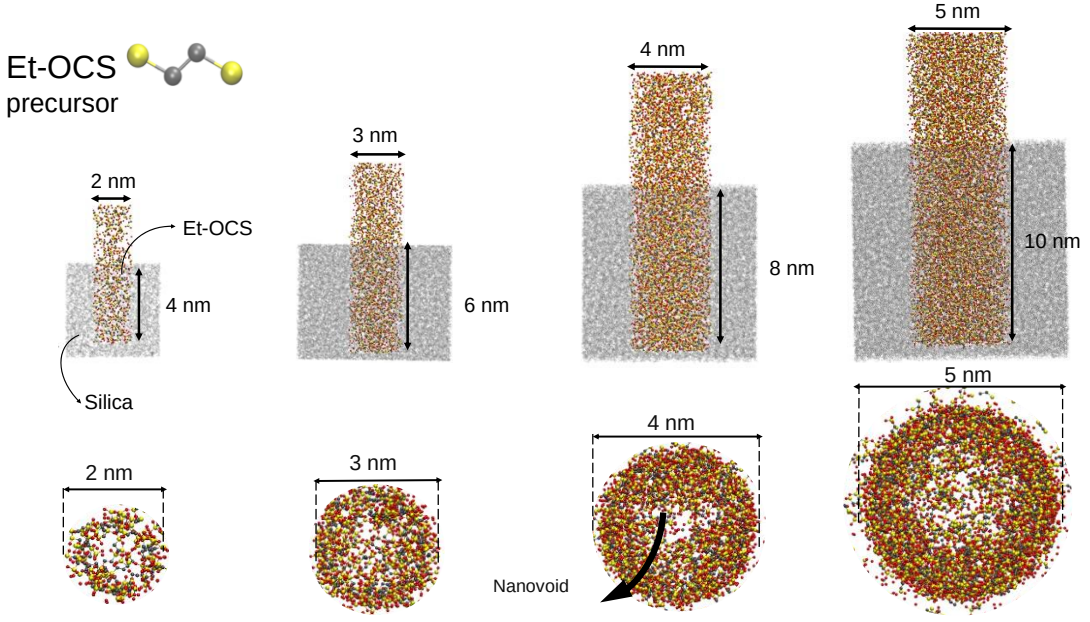

Stanford | ENGINEERING

Kilic et al., Computational Analysis of the Role of Nanoconfinement on the Reliability of ULK Glasses, *Proceedings of IEEE* (IITC), 2022.

12

Experimental Validation for Nanoconfinement Effects: Literature

Experimental Results

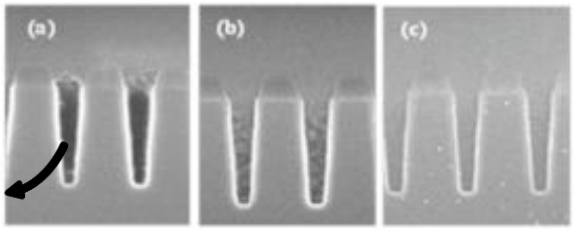

Void formation

Lee et al., Novel Flowable CVD Process Technology for sub-20nm Interlayer Dielectrics, IEEE.

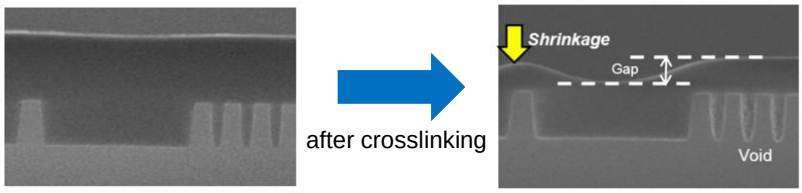

after crosslinking

Kobayashi et al., Plasma-Enhanced CVD Low-k Process Enabling Global Planarity by Controlling Flowability, IEEE, 2014

Simulation Results

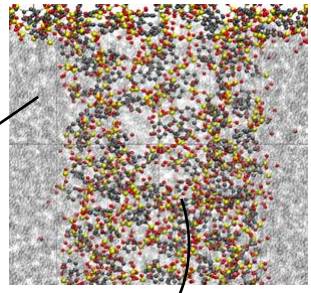

Silica (trench)

OSG filling

Et-OCS

"There is a need to provide alternative precursor compounds to produce silicon - containing films via flow CVD techniques…"

Ahner et al., Thermal stability and gap-fill properties of spin-on MSQ low-k dielectrics, Microelectronic Engineering, 2007

Sun et al.,STI Gap Fill Technology and Flowable CVD Process Application, IEEE.

Deng et al., New Applications and Challenges of Dielectric Films at 14 nm Finfet Technology and Beyond, IEEE.

Stanford | ENGINEERING

13

Analyzing Trench-Filling Sidewall Interactions

Strong Si-O interactions

Si-O bonding on the interface

Si-O bonds

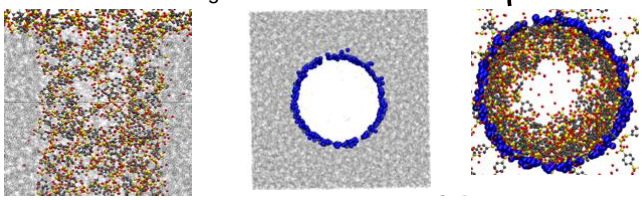

Weak Si-O interactions

No bonding on the interface

Atoms on the inner trench walls

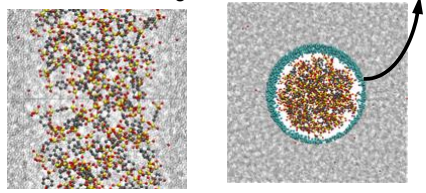

Trench – filling interaction gets weaker

Dimensions: 4 nm x 8 nm

4 nm

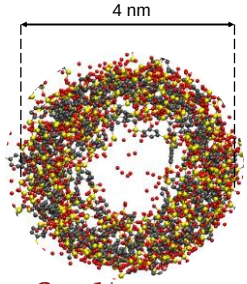

Dimensions: 4 nm x 8 nm

4 nm

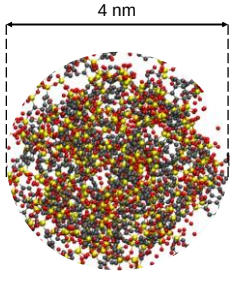

Dimensions: 4 nm x 8 nm

4 nm

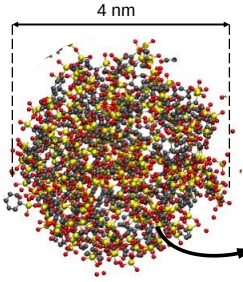

More material loss inside the gap!

OSG filling molecules accumulate towards the center when trench-filling interaction is weak, however less material remains inside the gap. Attractive interactions between trench and filling helps keep more material inside the gap despite the central void formation.

Stanford | ENGINEERING

14

The Role of Organosilicate Precursors

Gap dimensions: 4 nm x 8 nm (diameter x depth)

Et-OCS 

4 nm

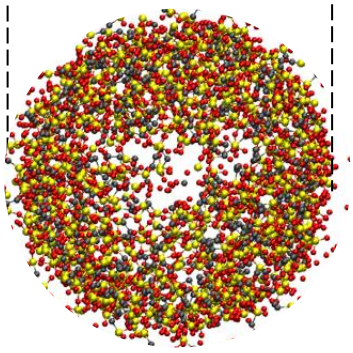

1,3,5-benzene 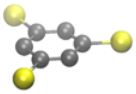

4 nm

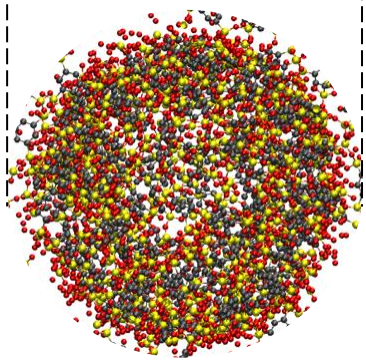

Suggested strategy to minimize nanovoid size: Use of precursors that interact effectively with one another to crosslink under confinement, such as the 1,3,5-benzene precursors

Stanford | ENGINEERING

Kilic et al., Computational Analysis of the Role of Nanoconfinement on the Reliability of ULK Glasses, *Proceedings of IEEE* (IITC), 2022.

15

Effects of Nanoconfinement on Elastic Properties

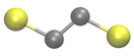 Et-OCS precursors

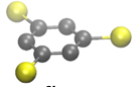 1,3,5-Benzene precursors

No confinement	Under confinement	No confinement	Under confinement
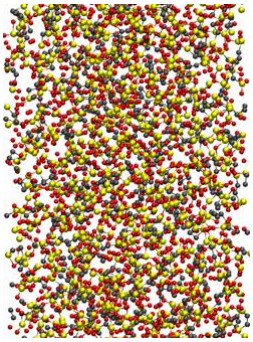	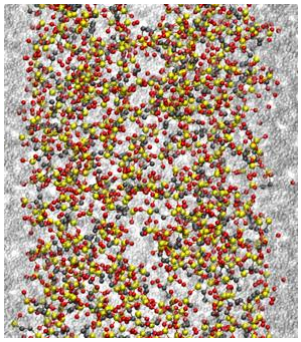	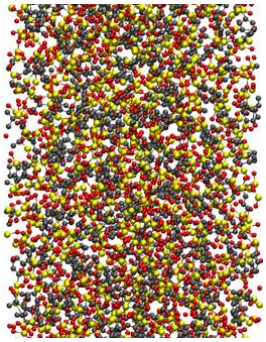	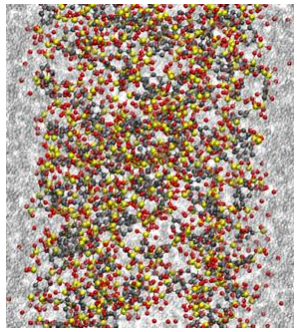
mSi = 3.4 Density = 1.6 g/cc Young's Modulus ~ 21 GPa	mSi = 2.88 Density = 1.05 g/cc **Young's Modulus ~ 2.5 GPa**	mSi = 4.4 Density = 1.8 g/cc Young's Modulus ~ 61 GPa	mSi = 3.62 Density = 1.13g/cc **Young's Modulus ~ 7.2 GPa**

1,3,5-benzene precursors form a stiffer network with better mechanical properties under nanoconfinement!

Stanford | ENGINEERING

Kilic et al., Computational Analysis of the Role of Nanoconfinement on the Reliability of ULK Glasses, *Proceedings of IEEE* (IITC), 2022.

16

Papers with Similar Experimental Results and Trends…

Device features: 25 nm width, 400 nm depth
Inner device walls are covered with silica
Filling material is mesoporous OSG

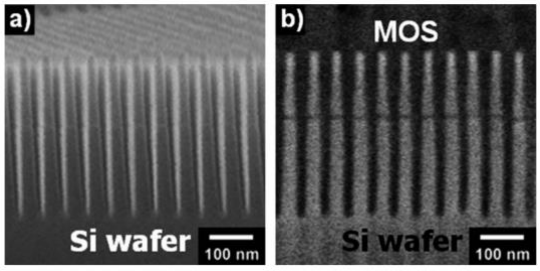

Device features: 2 nm width, 4 nm depth

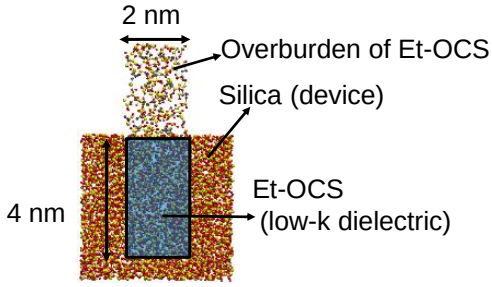

Final configuration has 53-56% porosity
Young's Modulus drops from
9 GPa to ~6 GPa

Our predictions for Young's Modulus are:
~ 2.5 GPa for Et-OCS and
~ 7.2 GPa for 1,3,5-Benzene

Stanford | ENGINEERING

Jang et al., Fabrication of mesoporous organosilica in a shallow nanotrench for low-k and high elastic modulus material application, Journal of Materials Chemistry, 2012.

17

Effects of Nanoconfinement on Fracture Properties

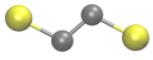

Et-OCS precursors

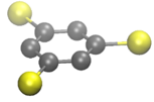

1,3,5-Benzene precursors

No confinement

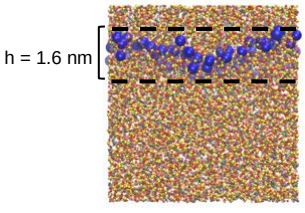

mSi = 3.4
Fracture bond density
1.9 nm^{-2}

Under confinement

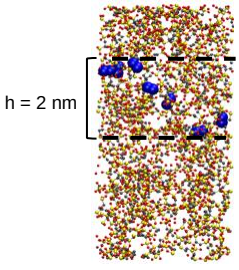

mSi = 2.88
Fracture bond density
0.24 nm^{-2}

No confinement

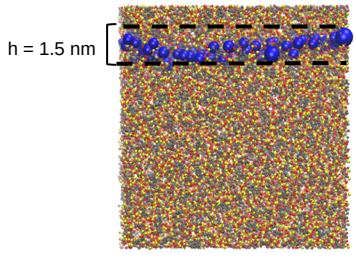

mSi = 4.4
Fracture bond density
2.5 nm^{-2}

Under confinement

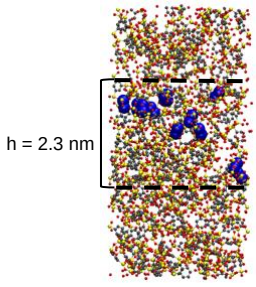

mSi = 3.62
Fracture bond density
0.35 nm^{-2}

1,3,5-benzene network has better fracture properties under confinement!

Stanford | ENGINEERING

Kilic et al., Computational Analysis of the Role of Nanoconfinement on the Reliability of ULK Glasses, *Proceedings of IEEE* (IITC), 2022.

18

Effects of Nanoconfinement on Fracture Properties

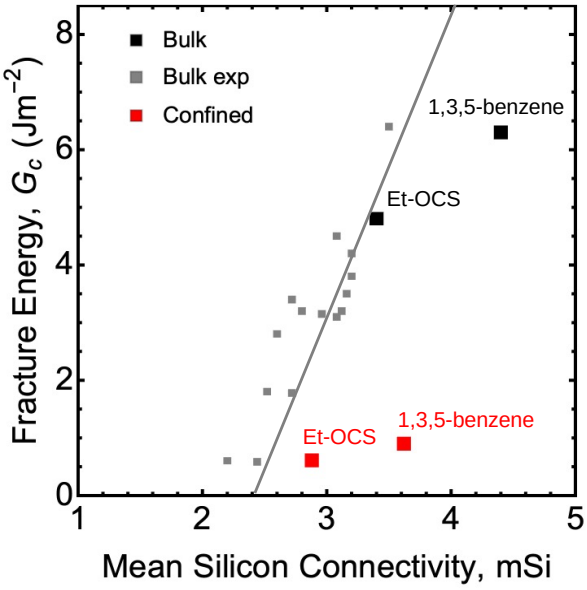

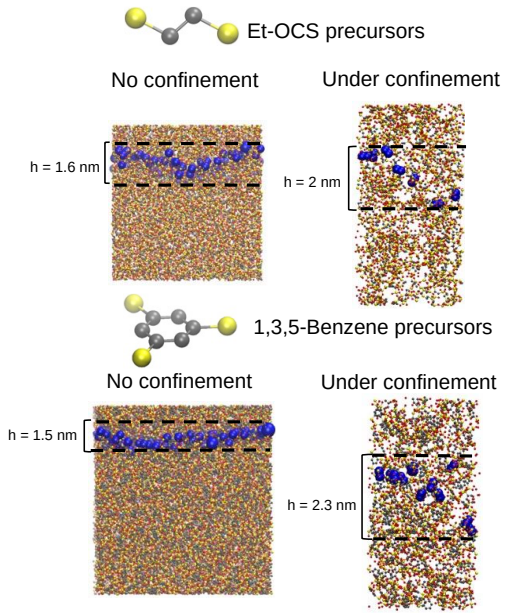

Stanford | ENGINEERING Oliver, M, et al, 2010 L. Wang et al, 2001 Y. Lin et al, 2008 F. Iacopi et al, 2007

19

ReaxFF for Effects of Moisture and Extreme Temperature

ReaxFF simulations capture the anomalous increase in silica stiffness with temperature

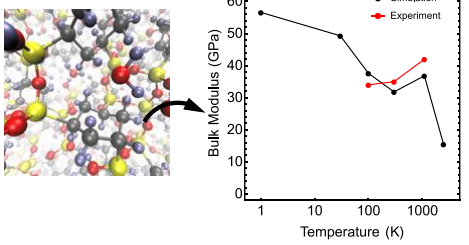

Fracture energies of nanoporous $SiCH_3$ networks in presence of moisture

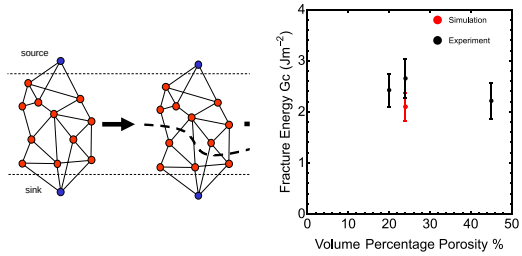

ReaxFF simulations show temperature dependant stiffness of OSG dielectrics

Absence of anomalous behavior seen in silica

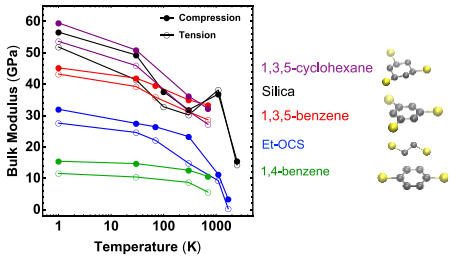

Min-cut algorithm for fracture path prediction including moisture effects

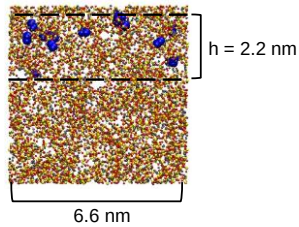

Stanford | ENGINEERING

20

Predicting Structure-Property Relationships with ML

Features (inputs)

Molecular features

Network Connectivity

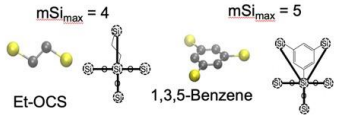

Precursor Geometry

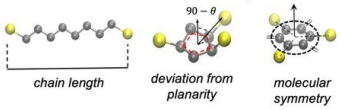

Macroscopic features

Porosity, condensation degree q, precursor fragmentation

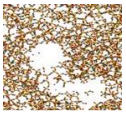

Outputs

Elastic Modulus, E "stiffness"

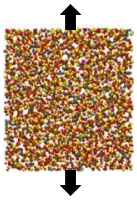

Fracture Energy, G_c "toughness"

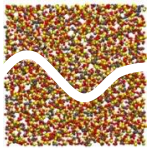

Design of Reliable low-k hybrids

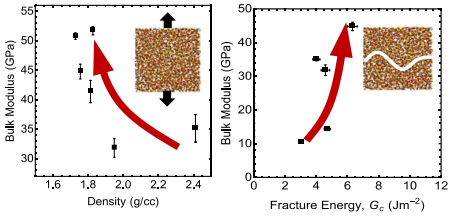

Machine Learning

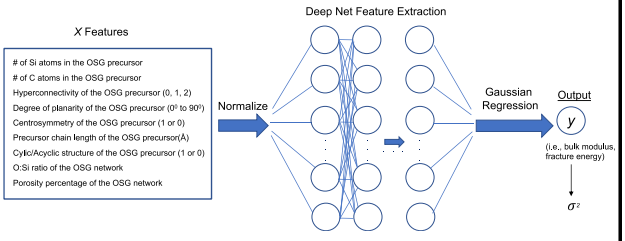

Stanford | ENGINEERING

21

Conclusion

Molecular structure

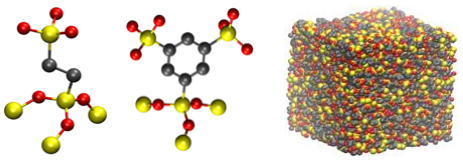

Precursor Geometry

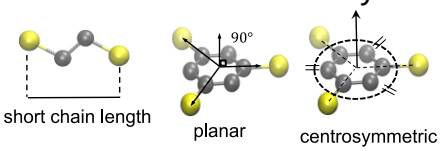

Nanoscale Confinement

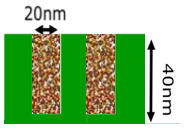

Mechanical properties

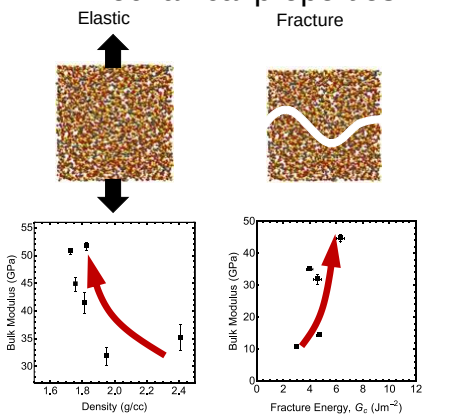

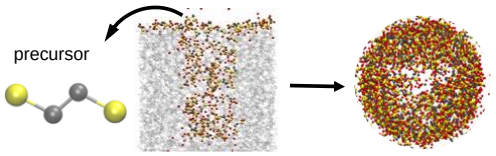

Stanford | ENGINEERING

22